Journal of Statistical Mechanics:
Theory and Experiment

PAPER

The Ising chain constrained to an even or odd number of positive spins

To cite this article: Michael T Gastner *J. Stat. Mech.* (2015) P03004

Journal of Statistical Mechanics: Theory and Experiment
An IOP and SISSA journal

The Ising chain constrained to an even or odd number of positive spins

Michael T Gastner

Institute of Technical Physics and Materials Science, Research Centre for Natural Sciences, Hungarian Academy of Sciences, PO Box 49, H-1525 Budapest, Hungary
Department of Engineering Mathematics, University of Bristol, Merchant Venturers Building, Woodland Road, Bristol BS8 1UB, UK
E-mail: m.gastner@bristol.ac.uk

Received 4 July 2014
Accepted for publication 5 February 2015
Published 3 March 2015

Online at stacks.iop.org/JSTAT/2015/P03004
doi:10.1088/1742-5468/2015/03/P03004

Abstract. We investigate the statistical mechanics of the periodic one-dimensional Ising chain when the number of positive spins is constrained to be either an even or an odd number. We calculate the partition function using a generalization of the transfer matrix method. On this basis, we derive the exact magnetization, susceptibility, internal energy, heat capacity and correlation function. We show that in general the constraints substantially slow down convergence to the thermodynamic limit. By taking the thermodynamic limit together with the limit of zero temperature and zero magnetic field, the constraints lead to new scaling functions and different probability distributions for the magnetization. We demonstrate how these results solve a stochastic version of the one-dimensional voter model.

Keywords: rigorous results in statistical mechanics, solvable lattice models

1742-5468/15/P03004+24$33.00

Contents

1. Introduction

For almost one century, the Ising model of ferromagnetism has been a cornerstone of statistical mechanics [1]. It is one of very few problems that can, at least in one and two dimensions, be solved exactly [2]. Its applications range from solid state physics [3] over neuroscience [4] to collective social phenomena [5]. In its basic form the Ising model is based on the Hamiltonian

$$E(\boldsymbol{\sigma}) = -J\sum_{i=1}^{N}\sigma_i\sigma_{i+1} - H\sum_{i=1}^{N}\sigma_i, \tag{1}$$

where each spin in the vector $\boldsymbol{\sigma} = (\sigma_1, \dots, \sigma_N)$ can take only the values ± 1 and we assume periodic boundary conditions so that $\sigma_{N+1} = \sigma_1$. The parameter J is the strength of interactions between spins and H an external magnetic field. We allow J to take positive and negative values, thereby considering both the ferro- and antiferromagnetic cases.

Many generalizations of the model have been investigated since Ising's groundbreaking publication, for example long-range interactions [6], spin glasses [7] and permitting more than two possible spin states [8]. In this article we investigate two different variations of the Ising model. First, we restrict the number of positive spins

$$N_+(\boldsymbol{\sigma}) = \frac{1}{2}\left(N + \sum_{i=1}^{N} \sigma_i\right) \quad (2)$$

to an even number. That is, the Hamiltonian is given by equation (1) if N_+ is even and $E = \infty$ if it is odd. In the second model, equation (1) holds if N_+ is odd, whereas an even N_+ is forbidden. We will refer to these two models as 'even' or 'odd' Ising model respectively[1].

In sections 2–4 we will motivate the even and odd models by showing that they are equivalent to a simple opinion formation model. In section 5 we demonstrate how the transfer matrix method for the unconstrained Ising model can be modified to derive the partition functions of the even and odd models. Section 6 contains a derivation of the magnetization and susceptibility of both models. We deduce the nearest-neighbour correlations, internal energy and heat capacity in section 7 and the correlation function in section 8. As we show in sections 9 and 10, the constrained models approach the thermodynamic limit in a different manner than the usual unconstrained model when the temperature and magnetic field simultaneously go to zero. We apply these results to the opinion formation model in section 11 before summarizing the key findings in section 12.

Before proceeding, we emphasize that N_+ is not a fixed number, neither in the even nor odd model. It is still permitted to take a multitude of values (e.g. in the even model $N_+ = 0, 2, 4, \ldots, 2\lfloor N/2 \rfloor$), but with the restriction that configurations with either odd or even N_+ are excluded. In a Monte Carlo simulation, this restriction could be imposed by initializing the spins with an even or odd N_+ and subsequently flipping two distinct spins simultaneously in each update. Because such a Markov chain is not ergodically exploring the configurations of the conventional (i.e. unconstrained) Ising model, we should not expect that the equilibrium properties are equal. One purpose of this article is to convince ourselves that the thermodynamic limits (i.e. $N \to \infty$) of the even and odd models are indeed the limits of the unconstrained model for fixed temperature. However, we will point out differences when the thermodynamic limit is taken simultaneously with the limit of zero temperature and zero magnetic field.

2. Motivation: stochastic synchronous voter model

We consider a version of the voter model with stochastic opinion updates. Individuals are placed on the N sites of a one-dimensional chain with periodic boundary conditions. Each individual holds one of two possible opinions: 'black' or 'white'. We associate each site i with a binary variable ω_i whose values are

$$\omega_i(t) = \begin{cases} 1 & \text{if } i \text{ is black at time } t, \\ -1 & \text{if } i \text{ is white at time } t. \end{cases} \quad (3)$$

At each discrete time step t, all individuals synchronously update their opinions [9]. (We will discuss asynchronous updates in section 4.) Each individual randomly chooses one of

[1] Sometimes the term 'odd Ising model' is used for a spin glass model by Villain [30] which is unrelated to our work.

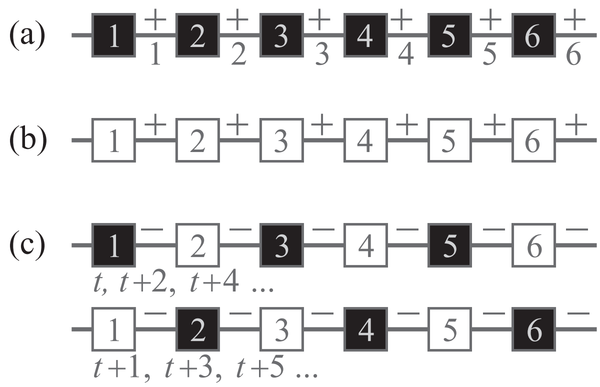

Figure 1. The (a), (b) stationary and (c) periodic states of the opinion dynamics of equation (4) in the limit $p_+ = 1$ with synchronous updates. A site i with $\omega_i = \pm 1$ is represented by a black (white) square. The spins of the associated Ising model are shown as $+$ or $-$ signs above the links.

their two nearest neighbours and adopts her opinion with probability p_+ or chooses the opposite opinion with probability $p_- = 1 - p_+$. Thus, the probability that i's next opinion is $\Omega = \pm 1$ can be expressed as

$$\Pr\left[\omega_i(t+1) = \Omega \,|\, \omega_{i-1}(t), \omega_{i+1}(t)\right] = \begin{cases} p_+ & \text{if } \frac{\Omega}{2}\left(\omega_{i-1}(t) + \omega_{i+1}(t)\right) = 1, \\ \frac{1}{2} & \text{if } \omega_{i-1}(t) + \omega_{i+1}(t) = 0, \\ p_- & \text{if } \frac{\Omega}{2}\left(\omega_{i-1}(t) + \omega_{i+1}(t)\right) = -1, \end{cases} \tag{4}$$

where the subindices are interpreted modulo N to satisfy the periodic boundary conditions.

What are the equilibrium properties of this model? For example, how many pairs of neighbours will on average disagree? And what are the typical fluctuations around this average value? We will demonstrate that these questions can be analytically answered by mapping the problem to an Ising model on the dual lattice with an even number of negative spins. (We will explain the origin of the even-numbered constraint in section 3.) For even (odd) N, the opinion model will consequently map onto the even (odd) Ising model.

Let us first clarify that the variables ω_i cannot directly be interpreted as Ising spins σ_i. For simplicity's sake, let us assume for a moment that N is even. In the limiting case of $p_+ = 1$, there are two stationary states where all sites have reached either a black or white consensus (figures 1(a) and (b)). For synchronous updates there is, however, also a periodic state where the opinions alternate in space [10]: if all odd sites are black and all even sites white at time t, all opinions are inverted at $t+1$ and return to the original state at $t+2$ (figure 1(c)). Unlike in the zero-temperature Ising model, we thus have apparently more than two ground states.

We can, however, establish a connection to the Ising model if we assign spins σ_i to the i-th link (i.e. between the sites i and $i+1$) rather than the sites themselves. We set $\sigma_i = 1$ if both sites connected by the link agree and $\sigma_i = -1$ if they disagree,

$$\sigma_i = \omega_i \omega_{i+1}. \tag{5}$$

In terms of σ_i, both consensus states are mapped to maximally positive magnetization, whereas in the alternating state all spins are negative. Thus, the limit $p_+ = 1$ can be mapped to the zero-temperature ferromagnetic Ising model. We will now argue that for any $0 < p_+ < 1$, there is a finite-temperature Ising model whose equilibrium properties are those of the original opinion dynamics given by equation (4).

3. Mapping the synchronous voter model to an odd or even Ising model

Suppose that the opinions at time t are $\omega_1^{(A)}, \ldots, \omega_N^{(A)}$. What is the probability $\Pr(A \to B)$ to find the opinions $\omega_1^{(B)}, \ldots, \omega_N^{(B)}$ at time $t+1$? Assuming that the probabilities in equation (4) are independent for all i,

$$\Pr(A \to B) = \prod_{i=1}^{N} \Pr\left[\omega_i^{(B)} \middle| \omega_{i-1}^{(A)}, \omega_{i+1}^{(A)}\right]. \tag{6}$$

We want to show that

$$\frac{\Pr(A \to B)}{\Pr(B \to A)} = \mathrm{e}^{\beta(E^{(A)} - E^{(B)})}, \tag{7}$$

where $E^{(A)}$ is the energy of the spins $\sigma_i^{(A)} = \omega_i^{(A)}\omega_{i+1}^{(A)}$ in the Ising model without magnetic field,

$$E^{(A)} = -J \sum_{i=1}^{N} \sigma_i^{(A)} \sigma_{i+1}^{(A)}, \tag{8}$$

and similarly for state B. Furthermore,

$$\beta = -\frac{\ln\left(2\sqrt{p_+ p_-}\right)}{2J} \tag{9}$$

so that every p_+ can be mapped to a temperature $(k_\mathrm{B}\beta)^{-1}$, where k_B is the Boltzmann constant. Equation (7) is the detailed balance condition for the Ising model [11]. Consequently, the equilibrium properties of the spins σ_i can be deduced from the model's partition function.

Before deriving equation (7), we emphasize that not all spin configurations are possible. The number of negative spins must be even; otherwise the opinions ω_i would change an odd number of times as we go once through the chain so that we would not end up with the same opinion with which we started. The restriction to an even number of negative spins changes the partition function of this model compared to the unconstrained Ising model.

First, however, we still need to justify equation (7). Let us denote the number of neighbouring spins with opposite signs in states A and B by $n^{(A)}$ and $n^{(B)}$ respectively. Because $E^{(A)} = J\left(2n^{(A)} - N\right)$ and $E^{(B)} = J\left(2n^{(B)} - N\right)$, we can rewrite the right-hand side of equation (7) as

$$\mathrm{e}^{\beta(E^{(A)} - E^{(B)})} = \mathrm{e}^{2\beta J(n^{(A)} - n^{(B)})}. \tag{10}$$

Because of equations (4) and (6), only factors p_+, $\frac{1}{2}$ and p_- can appear in $\Pr(A \to B)$ and $\Pr(B \to A)$,

$$\Pr(A \to B) = p_+^{a_1} p_-^{a_2} / 2^{a_3}, \tag{11}$$

$$\Pr(B \to A) = p_+^{b_1} p_-^{b_2} / 2^{b_3}. \tag{12}$$

J. Stat. Mech. (2015) P03004

Assuming $p_+ \neq \frac{1}{2}$, the exponents a_i, b_i are uniquely determined. (If $p_+ = \frac{1}{2}$ and thus $\beta = 0$, equation (7) is trivially correct.) There is one factor for each site, so

$$a_1 + a_2 + a_3 = b_1 + b_2 + b_3 = N. \tag{13}$$

Because $\sigma_i \sigma_{i+1} = -1$ if and only if $\omega_i + \omega_{i+2} = 0$, equation (4) implies

$$a_3 = n^{(A)}, \tag{14}$$

$$b_3 = n^{(B)}. \tag{15}$$

From equation (4) it also follows that

$$a_1 - a_2 = \frac{1}{2} \sum_i \omega_i^{(B)} \left(\omega_{i-1}^{(A)} + \omega_{i+1}^{(A)} \right), \tag{16}$$

$$b_1 - b_2 = \frac{1}{2} \sum_i \omega_i^{(A)} \left(\omega_{i-1}^{(B)} + \omega_{i+1}^{(B)} \right). \tag{17}$$

Splitting the sums and shifting the summation index shows that the sums in equations (16) and (17) are equal, thus

$$a_1 - a_2 = b_1 - b_2. \tag{18}$$

Combining equations (13)–(15) and (18),

$$a_2 = N - a_1 - n^{(A)}, \tag{19}$$

$$b_1 = a_1 + \frac{1}{2} \left(n^{(A)} - n^{(B)} \right), \tag{20}$$

$$b_2 = N - a_1 - \frac{1}{2} \left(n^{(A)} + n^{(B)} \right), \tag{21}$$

so that, by plugging into equations (11) and (12), we obtain

$$\frac{\Pr(A \to B)}{\Pr(B \to A)} = \left(2\sqrt{p_+ p_-} \right)^{n^{(B)} - n^{(A)}}. \tag{22}$$

Comparing equations (9), (10) and (22) proves equation (7).

4. The voter model with random asynchronous updates

Not only the voter model with perfectly synchronous updates of opinions can be mapped to an even or odd Ising model. We will now argue that, by defining the spins as in equation (5), we can also interpret asynchronous updates of randomly selected single opinions in terms of an Ising Hamiltonian. While the synchronous case, as shown in the previous section, corresponds to a positive spin interaction J and zero magnetic field H, the asynchronous case leads to $J = 0$ and, in general, $H \neq 0$ for the following reason.

Suppose opinion ω_i is chosen to be updated. The probability to have opinion Ω in the next time step is given by equation (4) while all other opinions remain unchanged. Then the only spins affected are σ_{i-1} and σ_i so that we can ignore the rest of the chain. If ω_i changes between states A and B, then we can distinguish the three cases depicted in figure 2: either

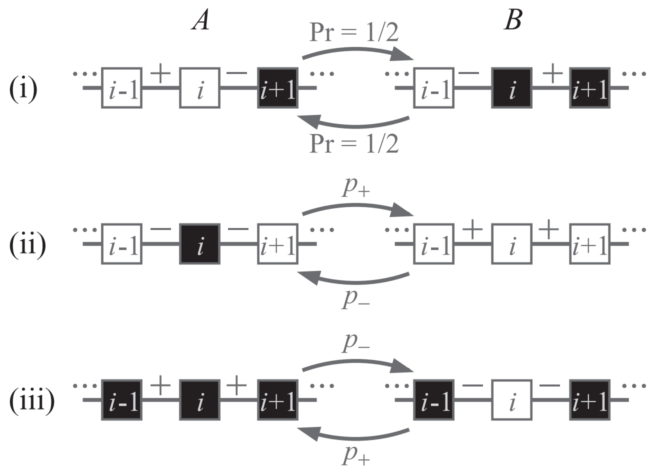

Figure 2. Transition probabilities for asynchronous updates. Depicted are three representative cases where only opinion i changes between states A and B. All other cases can be generated by inverting all opinions (from white to black and vice versa) and/or interchanging the order of the chain so that $i-1$ and $i+1$ trade places.

(i) $\Pr(A \to B) = \Pr(B \to A) = \frac{1}{2}$ and $\sigma_i^{(A)} + \sigma_{i+1}^{(A)} = \sigma_i^{(B)} + \sigma_{i+1}^{(B)} = 0$ or

(ii) $\Pr(A \to B) = p_+$ and $\Pr(B \to A) = p_-$ and $\sigma_i^{(A)} + \sigma_{i+1}^{(A)} = -\sigma_i^{(B)} - \sigma_{i+1}^{(B)} = -2$ or

(iii) $\Pr(A \to B) = p_-$ and $\Pr(B \to A) = p_+$ and $\sigma_i^{(A)} + \sigma_{i+1}^{(A)} = -\sigma_i^{(B)} - \sigma_{i+1}^{(B)} = 2$.

In summary, we can write all of these cases as

$$\frac{\Pr(A \to B)}{\Pr(B \to A)} = \left(\frac{p_+}{p_-}\right)^{-\frac{1}{4}\left(\sum \sigma_i^{(A)} - \sum \sigma_i^{(B)}\right)}, \tag{23}$$

which is of the form of equation (7) with the energy $E = -H\sum_i \sigma_i$ and inverse temperature

$$\beta = \frac{\ln(p_+/p_-)}{4H}. \tag{24}$$

If $p_+ \in (\frac{1}{2}, 1)$, we must have $H > 0$ to obtain a positive temperature. Asynchronous opinion updates then tend to favour the states depicted in figures 1(a) and (b) where the spins are all positive. Generally, the states in figure 1(c) are suppressed when $p_+ > 1/2$ and the dynamic rule mixes synchronous and asynchronous updates (e.g. by updating a fraction of the opinions in every update as in [12]). The opposite is true for $p_+ < 1/2$ where asynchronous updates generate sequences of alternating opinions and suppress unanimity. All cases, however, have in common that the periodic boundary conditions in the opinions generate an even number of negative spins, resulting in an even (odd) Ising model for even (odd) N.

Whether synchronous, asynchronous or partially synchronous updates are more realistic depends on the situation one wishes to model. Asynchronous updates have a long tradition in physics (e.g. the Glauber or Metropolis rules for dynamic Ising models),

J. Stat. Mech. (2015) P03004

but synchronous updates, especially in the context of stochastic cellular automata [13], have also been investigated (for example in [14–16]). If agents can only make decisions at discrete times (e.g. only at the end of a business day or if biological populations exhibit strongly peaked cyclic activity [17]), then synchronous or partially synchronous updates are more applicable. Here we do not intend to argue for any particular update rule. Generally, one has to be humble about social or economic interpretations of such simple rules [18] because true opinion dynamics is far more complex. Our focus here is rather on the model's structural properties in order to motivate how the even and odd Ising models can arise from another two-state model.

J. Stat. Mech. (2015) P03004

5. Partition function

We denote the partition function for the even and odd Ising model by Z_e and Z_o respectively,

$$Z_e = \sum_{\substack{\boldsymbol{\sigma} \text{ with} \\ \text{even } N_+(\boldsymbol{\sigma})}} \mathrm{e}^{-\beta E(\boldsymbol{\sigma})}, \tag{25}$$

$$Z_o = \sum_{\substack{\boldsymbol{\sigma} \text{ with} \\ \text{odd } N_+(\boldsymbol{\sigma})}} \mathrm{e}^{-\beta E(\boldsymbol{\sigma})}. \tag{26}$$

If we associate a spin $\sigma_i = 1$ with the bra vector $\langle +1| = (1, 0)$ and $\sigma_i = -1$ with $\langle -1| = (0, 1)$, we can write Z_e with the transfer matrix of the unconstrained model [19]

$$\mathbf{P} = \begin{pmatrix} \mathrm{e}^{\beta(J+H)} & \mathrm{e}^{-\beta J} \\ \mathrm{e}^{-\beta J} & \mathrm{e}^{\beta(J-H)} \end{pmatrix} \tag{27}$$

as

$$\begin{aligned} Z_e &= \sum_{\substack{\boldsymbol{\sigma} \text{ with} \\ \text{even } N_+(\boldsymbol{\sigma})}} \langle\sigma_1|\,\mathbf{P}\,|\sigma_2\rangle\,\langle\sigma_2|\,\mathbf{P}\,|\sigma_3\rangle \ldots \langle\sigma_N|\,\mathbf{P}\,|\sigma_1\rangle \\ &= \mathrm{Tr}\left(\sum_{\substack{\boldsymbol{\sigma} \text{ with} \\ \text{even } N_+(\boldsymbol{\sigma})}} |\sigma_1\rangle\,\langle\sigma_1|\,\mathbf{P} \ldots |\sigma_N\rangle\,\langle\sigma_N|\,\mathbf{P} \right). \end{aligned} \tag{28}$$

Similarly,

$$Z_o = \mathrm{Tr}\left(\sum_{\substack{\boldsymbol{\sigma} \text{ with} \\ \text{odd } N_+(\boldsymbol{\sigma})}} |\sigma_1\rangle\,\langle\sigma_1|\,\mathbf{P} \ldots |\sigma_N\rangle\,\langle\sigma_N|\,\mathbf{P} \right). \tag{29}$$

Let us define

$$\mathbf{M}_e = \sum_{\substack{\boldsymbol{\sigma} \text{ with} \\ \text{even } N_+(\boldsymbol{\sigma})}} |\sigma_1\rangle\,\langle\sigma_1|\,\mathbf{P} \ldots |\sigma_N\rangle\,\langle\sigma_N|\,\mathbf{P}, \tag{30}$$

$$\mathbf{M}_o = \sum_{\substack{\boldsymbol{\sigma} \text{ with} \\ \text{odd } N_+(\boldsymbol{\sigma})}} |\sigma_1\rangle\,\langle\sigma_1|\,\mathbf{P} \ldots |\sigma_N\rangle\,\langle\sigma_N|\,\mathbf{P}. \tag{31}$$

Induction on N proves

$$\begin{pmatrix} \mathbf{M}_e, & \mathbf{M}_o \\ \mathbf{M}_o, & \mathbf{M}_e \end{pmatrix} = \begin{pmatrix} |-1\rangle\langle -1|\,\mathbf{P}, & |+1\rangle\langle +1|\,\mathbf{P} \\ |+1\rangle\langle +1|\,\mathbf{P}, & |-1\rangle\langle -1|\,\mathbf{P} \end{pmatrix}^N . \tag{32}$$

With the definition

$$\mathbf{Q} = \begin{pmatrix} |-1\rangle\langle -1|\,\mathbf{P}, & |+1\rangle\langle +1|\,\mathbf{P} \\ |+1\rangle\langle +1|\,\mathbf{P}, & |-1\rangle\langle -1|\,\mathbf{P} \end{pmatrix} \tag{33}$$

$$= \begin{pmatrix} 0 & 0 & \mathrm{e}^{\beta(J+H)} & \mathrm{e}^{-\beta J} \\ \mathrm{e}^{-\beta J} & \mathrm{e}^{\beta(J-H)} & 0 & 0 \\ \mathrm{e}^{\beta(J+H)} & \mathrm{e}^{-\beta J} & 0 & 0 \\ 0 & 0 & \mathrm{e}^{-\beta J} & \mathrm{e}^{\beta(J-H)} \end{pmatrix},$$

we can write

$$Z_e = \mathrm{Tr}\left(\mathbf{M}_e\right) = \frac{1}{2}\mathrm{Tr}\left(\mathbf{Q}^N\right). \tag{34}$$

To simplify the notation further, we introduce

$$x = \beta H, \tag{35}$$

$$y = \beta J. \tag{36}$$

The eigenvalues of $\mathbf{Q}$ are then

$$\lambda_{1,2} = \mathrm{e}^y\left(\cosh x \pm \sqrt{\sinh^2 x + \mathrm{e}^{-4y}}\right), \tag{37}$$

$$\lambda_{3,4} = \mathrm{e}^y\left(-\sinh x \pm \sqrt{\cosh^2 x - \mathrm{e}^{-4y}}\right). \tag{38}$$

Consequently,

$$Z_e = \frac{1}{2}\left(\lambda_1^N + \lambda_2^N + \lambda_3^N + \lambda_4^N\right). \tag{39}$$

We can derive Z_o as follows. The eigenvalues $\lambda_{1,2}$ are also the eigenvalues of $\mathbf{P}$ and therefore the partition function of the unconstrained Ising model is $Z_u = \lambda_1^N + \lambda_2^N$. Moreover $Z_u = Z_e + Z_o$ so that

$$Z_o = \frac{1}{2}\left(\lambda_1^N + \lambda_2^N - \lambda_3^N - \lambda_4^N\right). \tag{40}$$

Because λ_1 is the leading eigenvalue, we find in the thermodynamic limit (i.e. $N \to \infty$) with fixed x and y that $Z_e \propto Z_o \propto Z_u \propto \lambda_1^N$. As a consequence, all equilibrium properties of the even and odd Ising models converge to the same limits as the unconstrained model. However, we will analytically derive in section 9 different scaling limits for $N \to \infty$ when temperature and magnetic field go to their critical value (i.e. zero) such that $N\mathrm{e}^{-2y}$ and $N \sinh x$ are asymptotically constants. For this purpose, it will be instructive to derive first some exact formulae for finite N.

6. Magnetization and susceptibility

We first calculate the mean magnetization per spin

$$\langle m\rangle \equiv \frac{\langle\sum_i \sigma_i\rangle}{N} = \frac{1}{N}\frac{\partial}{\partial x}\ln Z, \tag{41}$$

where Z is the partition function of the model in question and the angle brackets denote the ensemble average. With the auxiliary functions

$$s_1(x, y) = \frac{\sinh x}{\sqrt{\sinh^2 x + \mathrm{e}^{-4y}}}, \tag{42}$$

$$c_1(x, y) = \frac{\cosh x}{\sqrt{\cosh^2 x - \mathrm{e}^{-4y}}}, \tag{43}$$

we can write equation (41) as

$$\langle m \rangle_{e,o}(x, y) = \frac{s_1 \left(\lambda_1^N - \lambda_2^N\right) \mp c_1 \left(\lambda_3^N - \lambda_4^N\right)}{\lambda_1^N + \lambda_2^N \pm \lambda_3^N \pm \lambda_4^N}, \tag{44}$$

where the upper signs apply to the even and the lower signs to the odd model.

In the special case $x = 0$, applicable to the synchronous voter model, we insert the eigenvalues from equations (37) and (38) (figure 3(a))

$$\langle m \rangle_{e,o}(x = 0, y) = \begin{cases} \langle m \rangle_u(x = 0, y) = 0 & \text{if } N \text{ is even,} \\ \mp \frac{e^y}{\cosh^N y + \sinh^N y} \left(\frac{\sinh(2y)}{2}\right)^{(N-1)/2} & \text{if } N \text{ is odd.} \end{cases} \tag{45}$$

Hence, for odd N, even when there is no external magnetic field (i.e. $H = 0$), the magnetization is generally different from zero. This phenomenon can be intuitively explained. The constraint of an even number of positive spins prevents for odd N a ground state with perfectly aligned positive spins. However, the state with $\sigma_1 = \ldots = \sigma_N = -1$ is permitted and therefore the mean magnetization in the limit $y \to \infty$ is -1. The same argument applies with opposite signs to the odd model. In the antiferromagnetic limit (i.e. $y \to -\infty$) the neighbouring spins prefer to be in opposite directions, but an odd N forces at least one pair to point in the same direction and thus $m_{e,o} = (-1)^{(N\pm1)/2}/N$.

The relevant case for the asynchronous voter model is $y = 0$ where the interactions between spins are negligible compared to the external magnetic field,

$$\langle m \rangle_{e,o}(x, y = 0) = \frac{\sinh(2x)}{2} \times \frac{\cosh^{N-2} x \pm (-1)^N \sinh^{N-2} x}{\cosh^N x \pm (-1)^N \sinh^N x}. \tag{46}$$

The functions are plotted in figures 3(b) and (c). In the unconstrained model the magnetization $\langle m \rangle_u(x, y = 0) = \tanh x$ is independent of N. However, in the even and odd models, the constraints on the number of spins acts as an effective interaction so that the partition function does not factorize although $J = 0$. Consequently, the magnetization of equation (46) depends on N.

The fluctuations in the magnetization are measured by the susceptibility per spin

$$\chi \equiv \beta N \left(\langle m^2 \rangle - \langle m \rangle^2\right) = \frac{\partial \langle m \rangle}{\partial H}. \tag{47}$$

Taking the derivative of equation (44) for general x and y is in principle possible, but leads to rather lengthy expressions. We focus here instead directly on the two special cases $x = 0$ and $y = 0$.

J. Stat. Mech. (2015) P03004

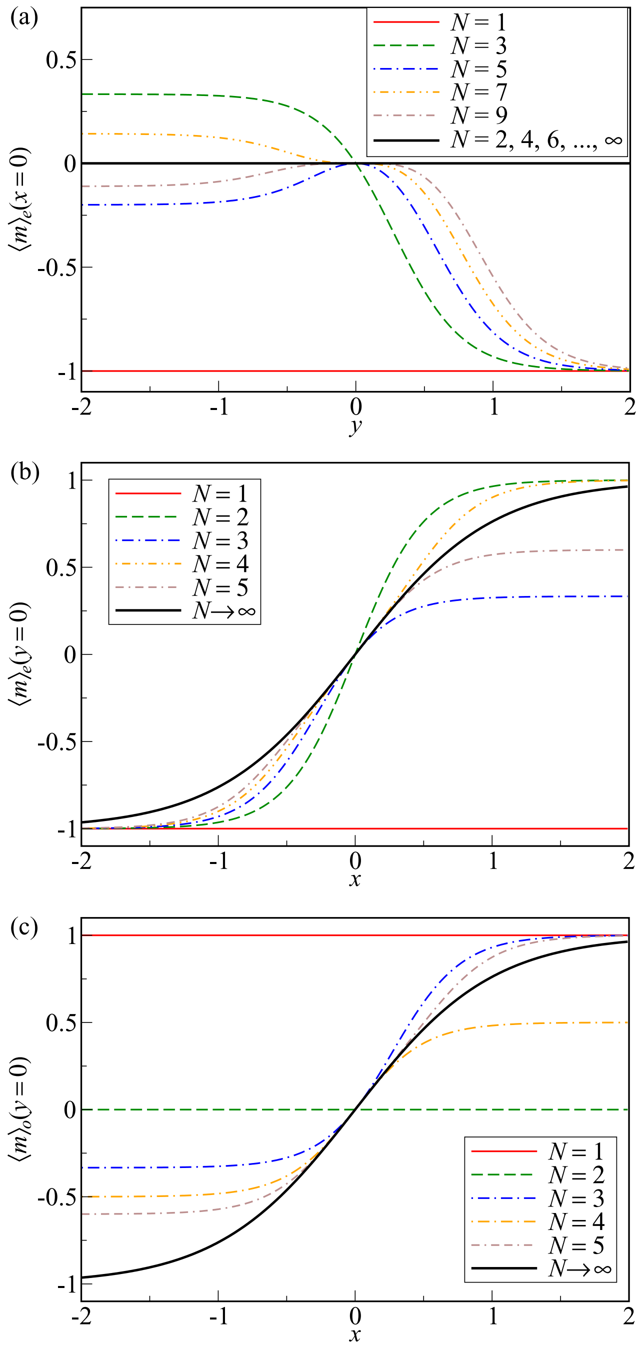

Figure 3. The mean magnetization $\langle m_e \rangle$ (a) as a function of y when $x = 0$, (b) as a function of x when $y = 0$. (c) The mean magnetization $\langle m_o \rangle$ for $y = 0$.

For $x = 0$ (i.e. in the absence of an external magnetic field),

$$\chi_{e,o}(x=0,y) = \begin{cases} \dfrac{\beta \mathrm{e}^{2y}\left(\cosh^N y - \sinh^N y \pm 2^{-N/2} N \sinh^{N/2-1}(2y)\right)}{\left(\cosh^{N/2} y \pm \sinh^{N/2} y\right)^2} & \text{if } N \text{ is even,} \\ \dfrac{\beta \mathrm{e}^{2y}\left(\cosh^{2N} y - \sinh^{2N} y - 2^{1-N} N \sinh^{N-1}(2y)\right)}{\left(\cosh^N y + \sinh^N y\right)^2} & \text{if } N \text{ is odd,} \end{cases} \quad (48)$$

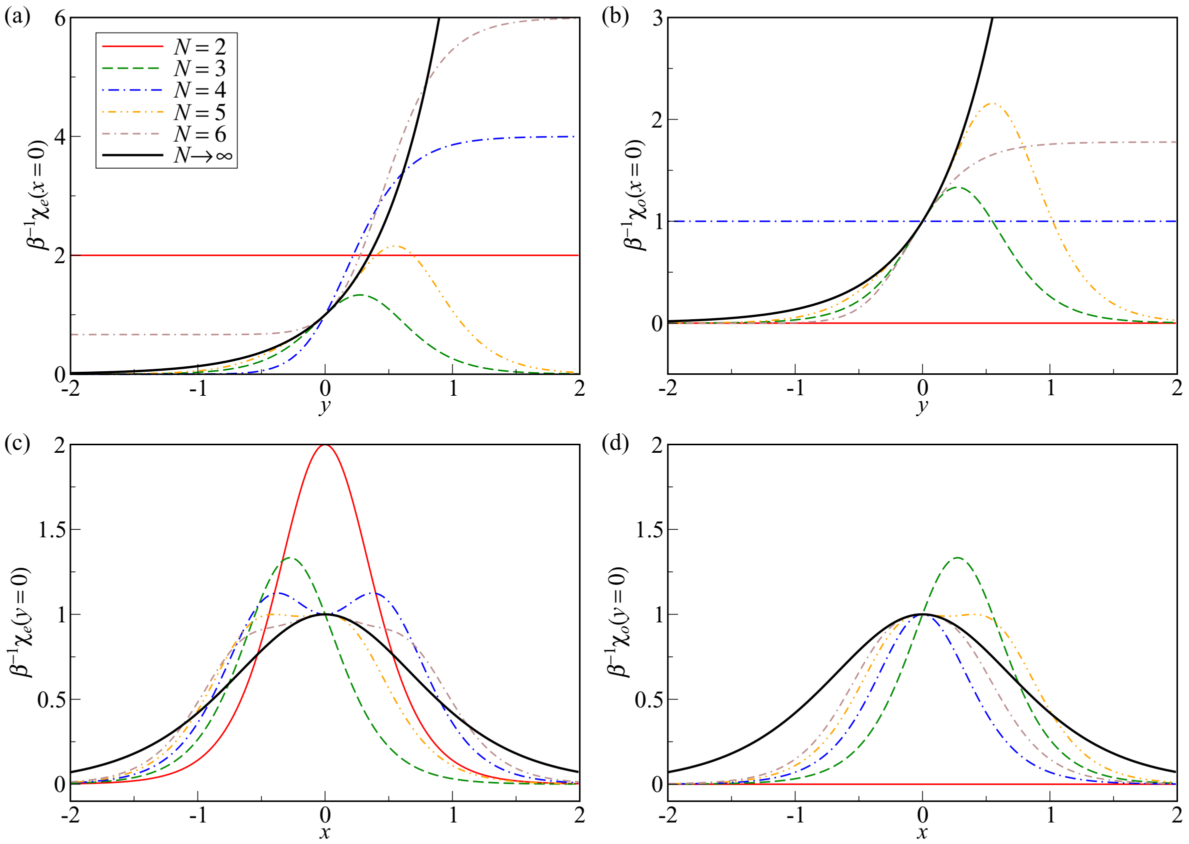

Figure 4. The susceptibility χ divided by the inverse temperature β for (a), (b) zero magnetic field H as a function of $y = \beta J$ and (c), (d) zero spin interaction J as a function of $x = \beta H$. Panels (a) and (c) show the results for the even Ising model, (b) and (d) for the odd model.

compared to $\chi_u = \beta e^{2y}(\cosh^N y - \sinh^N y)/(\cosh^N y + \sinh^N y)$. Plotting $\chi_{e,o}$ in figures 4(a) and (b), the most striking feature for odd N is $\lim_{y\to\infty} \chi_{e,o} = 0$, whereas the unconstrained Ising model (and the even model for even N) reaches in this limit its maximum susceptibility βN. The reason is that, as already mentioned, the even and odd models for odd N only have one ground state each, but the unconstrained model has two.

For the odd model with even N we observe yet another interesting phenomenon. The susceptibility reaches its maximum in the limit $y \to \infty$, but with a smaller value than the unconstrained or even models, namely $\lim_{y\to\infty} \chi_o = \beta(N^2 - 4)/(3N)$. The explanation is that the perfectly aligned ground states of the unconstrained models are not permitted. Therefore, the states of minimum energy in the odd model are the first excited states of the unconstrained model whose magnetization is not confined to the extreme values $m = \pm 1$.

In the case of no internal interactions (i.e. $y = 0$),

$$\chi_{e,o}(x, y = 0) = \beta \left(\frac{\cosh^{N-2} x \mp (-1)^N \sinh^{N-2} x}{\cosh^N x \pm (-1)^N \sinh^N x} \pm \frac{(-1)^N N \sinh^{N-2}(2x)}{2^{N-2}\left(\cosh^N x \pm (-1)^N \sinh^N x\right)^2} \right), \tag{49}$$

J. Stat. Mech. (2015) P03004

while $\chi_u = \beta\cosh^{-2} x$. We plot $\chi_{e,o}$ in figures 4(*c*) and (*d*). For odd N, they satisfy $\chi_e(x,0) = \chi_o(-x,0)$ because in this case the odd model is equivalent to the even model with flipped signs of spins and magnetic field. If N is even, χ_e and χ_o are intrinsically symmetric, but with larger values in the tails of the even model because $\chi_e/\chi_o \to 3N/(N-2)$ as $|x| \to \infty$ and $y = 0$.

7. Nearest-neighbour correlations, internal energy and heat capacity

If we replace in equation (41) the partial derivative with respect to x by differentiation with respect to y, we obtain the mean nearest-neighbour correlation

$$\langle g_1\rangle \equiv \frac{1}{N}\left\langle \sum_i \sigma_i\sigma_{i+1}\right\rangle = \frac{1}{N}\frac{\partial}{\partial y}\ln Z. \tag{50}$$

If we define the functions

$$s_2(x,y) = 2\mathrm{e}^{-3y}\left(\sinh^2 x + \mathrm{e}^{-4y}\right)^{-1/2}, \tag{51}$$

$$c_2(x,y) = 2\mathrm{e}^{-3y}\left(\cosh^2 x - \mathrm{e}^{-4y}\right)^{-1/2}, \tag{52}$$

then

$$\langle g_1\rangle_{e,o}(x,y) = 1 + \frac{s_2\left(\lambda_2^{N-1} - \lambda_1^{N-1}\right) \pm c_2\left(\lambda_3^{N-1} - \lambda_4^{N-1}\right)}{\lambda_1^N + \lambda_2^N \pm \lambda_3^N \pm \lambda_4^N}. \tag{53}$$

Without external magnetic field,

$$\langle g_1\rangle_{e,o}(x=0,y) = \begin{cases} 1 - \frac{\cosh^{N/2-1} y \mp \sinh^{N/2-1} y}{e^y\left(\cosh^{N/2} y \pm \sinh^{N/2} y\right)} & \text{if } N \text{ is even,} \\ \langle g_1\rangle_u(x=0,y) = 1 + \frac{\sinh^{N-1} y - \cosh^{N-1} y}{e^y\left(\cosh^N y + \sinh^N y\right)} & \text{if } N \text{ is odd.}\end{cases} \tag{54}$$

If N is odd, $\langle g_1\rangle_{e,o}(x=0,y)$ is equal to the correlation in the unconstrained model for the following reason. The spin configurations in the unconstrained model can be divided into two sets: one set containing all configurations of the even model and another set with all odd-numbered states. We can map every element in one set uniquely to the configuration in the other set that has all spins inverted. Because the sum of equation (50) is invariant if all spins are simultaneously flipped, the average correlations must be equal in both sets. The same argument cannot be applied to even N, however, because inverting the spins in the even or odd set generates another spin in the same set. As a consequence, $\langle g_1\rangle_e$ and $\langle g_1\rangle_o$ are in this case different functions.

With a magnetic field, but with vanishing spin interactions,

$$\langle g_1\rangle_{e,o}(x,y=0) = 1 - \frac{\cosh^{N-2} x \mp (-1)^N \sinh^{N-2} x}{\cosh^N x \pm (-1)^N \sinh^N x}, \tag{55}$$

compared to $\langle g_1\rangle_u = \tanh^2 x$. For odd N, we find $\langle g_1\rangle_e(x,0) = \langle g_1\rangle_o(-x,0)$ for the same reason as discussed after the corresponding equation (49) for the susceptibility. We also find again that, for even N, $\langle g_1\rangle_e(x,0) = \langle g_1\rangle_e(-x,0)$ and $\langle g_1\rangle_o(x,0) = \langle g_1\rangle_o(-x,0)$. Expanding equation (55), however, shows that the limits for $|x| \to \infty$ and even N are different: $\langle g_1\rangle_e \to 1$, but $\langle g_1\rangle_o \to 1-4/N$. The intuition behind this result is that a strong magnetic field can perfectly align the spins in the even, but not in the odd model.

J. Stat. Mech. (2015) P03004

Closely related to the nearest-neighbour correlations is the internal energy (i.e. ensemble average of the Hamiltonian) per spin

$$U \equiv \frac{\langle E \rangle}{N} = -\frac{1}{N}\frac{\partial}{\partial \beta} \ln Z. \tag{56}$$

In general, the calculation yields rather lengthy expressions. However, if $H = 0$, then $U_{e,o} = -J\langle g_1 \rangle_{e,o}(x = 0, y)$. If, on the other hand, J vanishes, then $U_{e,o} = -H\langle m \rangle_{e,o}(x, y = 0)$. Using our earlier results of equations (46) and (54),

$$U_{e,o}(x=0,y) = \begin{cases} J\left(\frac{\cosh^{N/2-1} y \mp \sinh^{N/2-1} y}{e^y\left(\cosh^{N/2} y \pm \sinh^{N/2} y\right)} - 1\right) & \text{if } N \text{ is even,} \\ U_u(x=0,y) = J\left(\frac{\cosh^{N-1} y - \sinh^{N-1} y}{e^y\left(\cosh^{N} y + \sinh^{N} y\right)} - 1\right) & \text{if } N \text{ is odd,} \end{cases} \tag{57}$$

$$U_{e,o}(x, y=0) = -\frac{H\sinh(2x)}{2} \times \frac{\cosh^{N-2} x \pm (-1)^N \sinh^{N-2} x}{\cosh^N x \pm (-1)^N \sinh^N x}., \tag{58}$$

while $U_u(x, y = 0) = -H \tanh x$.

Taking another derivative of $\ln Z$ with respect to β gives us the heat capacity per spin, which measures the fluctuations in the energy,

$$C \equiv \frac{k_B \beta^2}{N}\left(\langle E^2 \rangle - \langle E \rangle^2\right) = -k_B \beta^2 \frac{\partial U}{\partial \beta} \tag{59}$$

For vanishing H, we can use $(\partial U)/(\partial\beta) = J(\partial U)/(\partial y)$ and equation (57). If $J = 0$, then $C = k_B \beta H^2 \chi$, so the heat capacity follows directly from equation (49),

$$\begin{aligned} C_{e,o}(x=0,y) & \\ = \begin{cases} \dfrac{k_B\beta^2 J^2}{\cosh^{N/2} y \pm \sinh^{N/2} y} \\ \quad \times \left(\cosh^{N/2-2} y \mp \sinh^{N/2-2} y \pm \frac{N\sinh^{N/2-2}(2y)}{2^{N/2-1}\left(\cosh^{N/2} y \pm \sinh^{N/2} y\right)}\right) & \text{if } N \text{ is even,} \\ C_u(x=0,y) = \frac{k_B\beta^2 J^2}{\cosh^N y + \sinh^N y} \\ \quad \times \left(\cosh^{N-2} y - \sinh^{N-2} y + \frac{N\sinh^{N-2}(2y)}{2^{N-2}\left(\cosh^N y + \sinh^N y\right)}\right) & \text{if } N \text{ is odd,} \end{cases} \end{aligned} \tag{60}$$

$$\begin{aligned} &C_{e,o}(x, y=0) \\ &= k_B\beta^2 H^2 \left(\frac{\cosh^{N-2} x \mp (-1)^N \sinh^{N-2} x}{\cosh^N x \pm (-1)^N \sinh^N x} \pm \frac{(-1)^N N \sinh^{N-2}(2x)}{2^{N-2}\left(\cosh^N x \pm (-1)^N \sinh^N x\right)^2}\right), \end{aligned} \tag{61}$$

approaching $C_u(x, y = 0) = k_B\beta^2 H^2 \cosh^{-2}(x)$ in the thermodynamic limit.

8. Correlation function

We can generalize the calculation in the previous section to find the correlation between k-th nearest neighbours. For this purpose we make the spin interactions J in an auxiliary

Hamiltonian $\tilde{E}$ dependent on the position i, but for simplicity's sake we drop the magnetic field,

$$\tilde{E}(\boldsymbol{\sigma}) = -\sum_{i=1}^{N} J_i\sigma_i\sigma_{i+1}. \tag{62}$$

Applying the same line of reasoning that led us to equation (34), we can show that the partition function for the Hamiltonian $\tilde{E}$ in the case of even N^+ is

$$\tilde{Z}_e = \frac{1}{2}\mathrm{Tr}\left(\prod_{i=1}^{N}\mathbf{Q}_i\right), \tag{63}$$

where

$$\mathbf{Q}_i = \begin{pmatrix} 0 & 0 & \mathrm{e}^{\beta J_i} & \mathrm{e}^{-\beta J_i} \\ \mathrm{e}^{-\beta J_i} & \mathrm{e}^{\beta J_i} & 0 & 0 \\ \mathrm{e}^{\beta J_i} & \mathrm{e}^{-\beta J_i} & 0 & 0 \\ 0 & 0 & \mathrm{e}^{-\beta J_i} & \mathrm{e}^{\beta J_i} \end{pmatrix} \tag{64}$$

plays the role of the transfer matrix of equation (33). The matrices $\mathbf{Q}_i$ do not commute and therefore we cannot simultaneously diagonalize them for computing the trace in equation (63). However, the product $\mathbf{Q}_i\mathbf{Q}_{i+1}$ commutes with $\mathbf{Q}_{i+2}\mathbf{Q}_{i+3}$. These products are diagonalized as $\mathbf{R}\mathbf{Q}_i\mathbf{Q}_{i+1}\mathbf{R}$ by the matrix of eigenvectors

$$\mathbf{R} = \frac{1}{2}\begin{pmatrix} 1 & 1 & 1 & 1 \\ 1 & -1 & 1 & -1 \\ 1 & 1 & -1 & -1 \\ 1 & -1 & -1 & 1 \end{pmatrix} = \mathbf{R}^{-1}, \tag{65}$$

and the corresponding eigenvalues are

$$(\mathbf{R}\mathbf{Q}_i\mathbf{Q}_{i+1}\mathbf{R})_{11} = 4\cosh(\beta J_i)\cosh(\beta J_{i+1}), \tag{66}$$

$$(\mathbf{R}\mathbf{Q}_i\mathbf{Q}_{i+1}\mathbf{R})_{22} = 4\sinh(\beta J_i)\sinh(\beta J_{i+1}), \tag{67}$$

$$(\mathbf{R}\mathbf{Q}_i\mathbf{Q}_{i+1}\mathbf{R})_{33} = 4\sinh(\beta J_i)\cosh(\beta J_{i+1}), \tag{68}$$

$$(\mathbf{R}\mathbf{Q}_i\mathbf{Q}_{i+1}\mathbf{R})_{44} = 4\cosh(\beta J_i)\sinh(\beta J_{i+1}). \tag{69}$$

If N is even, it follows that

$$\begin{aligned}\tilde{Z}_{e,\text{even } N} = 2^{N-1}\Bigg(&\prod_{i=1}^{N}\cosh(\beta J_i) + \prod_{i=1}^{N}\sinh(\beta J_i) \\ &+ \prod_{i=1}^{N/2}\cosh(\beta J_{2i-1})\sinh(\beta J_{2i}) + \prod_{i=1}^{N/2}\sinh(\beta J_{2i-1})\cosh(\beta J_{2i})\Bigg),\end{aligned} \tag{70}$$

while for odd N the partition function is half of the unconstrained model's partition function

$$\tilde{Z}_{e,\text{odd } N} = \frac{1}{2}\tilde{Z}_u = 2^{N-1}\left(\prod_{i=1}^{N}\cosh(\beta J_i) + \prod_{i=1}^{N}\sinh(\beta J_i)\right). \tag{71}$$

doi:10.1088/1742-5468/2015/03/P03004

J. Stat. Mech. (2015) P03004

For the odd model, we can apply $\tilde{Z}_o = \tilde{Z}_u - \tilde{Z}_e$. The disconnected correlation function $\langle g_k \rangle$ can now be computed as

$$\langle g_k \rangle = \frac{1}{N} \left\langle \sum_i \sigma_i \sigma_{i+k} \right\rangle = \left[\frac{1}{\beta^k \tilde{Z}} \frac{\partial}{\partial J_1} \frac{\partial}{\partial J_2} \cdots \frac{\partial}{\partial J_k} \tilde{Z} \right]_{J_1 = \ldots = J_N = J} \tag{72}$$

with the final result

$$\langle g_k \rangle_{e,o} = \begin{cases} \frac{\cosh^{N-k} y \sinh^k y + \sinh^{N-k} y \cosh^k y \pm 2^{1-N/2} \cosh(2y) \sinh^{N/2-1}(2y)}{\left(\cosh^{N/2} y \pm \sinh^{N/2} y\right)^2} & \text{if } N \text{ even}, \ k \text{ odd}, \\ \frac{\cosh^{N-k} y \sinh^k y + \sinh^{N-k} y \cosh^k y \pm 2^{1-N/2} \sinh^{N/2}(2y)}{\left(\cosh^{N/2} y \pm \sinh^{N/2} y\right)^2} & \text{if } N \text{ even}, \ k \text{ even}, \\ \langle g_k \rangle_u = \frac{\cosh^{N-k} y \sinh^k y + \sinh^{N-k} y \cosh^k y}{\cosh^N y + \sinh^N y} & \text{if } N \text{ odd}. \end{cases} \tag{73}$$

Taking the limit $N \to \infty$ while keeping y and k fixed, all three cases have the same asymptotic value $\lim_{N\to\infty} \langle g_k \rangle_{e,o,u} = \tanh^k y$ and the correlation length is hence $\xi = -\ln(\tanh y)$. The divergence at $y = 0$ can be expressed as a power law in the reduced temperature [20]

$$T_{\mathrm{r}} = \mathrm{e}^{-2y} \tag{74}$$

because near $T_{\mathrm{r}} = 0$

$$\xi \approx 2T_{\mathrm{r}}^{-1} \propto T_{\mathrm{r}}^{-\nu}, \tag{75}$$

where the critical correlation length exponent satisfies $\nu = 1$ in the unconstrained, even and odd models.

9. Approach to the thermodynamic limit

It is not surprising that ν does not depend on whether we constrain the number of positive spins to even or odd values or have no such constraint. We have already pointed out the reason after equation (40): the thermodynamic limit at fixed temperature is determined by the leading eigenvalue λ_1 and this eigenvalue is common to the transfer matrices $\mathbf{P}$ and $\mathbf{Q}$. The leading-order correction to the magnetization, however, depends on the eigenvalue with the second largest absolute value. If we call this eigenvalue λ_s, then the average magnetization for a chain of length N behaves asymptotically as

$$\langle m \rangle = s_1 + \left(\frac{\lambda_s}{\lambda_1}\right)^{N-1} \frac{\partial}{\partial x} \left(\frac{\lambda_s}{\lambda_1}\right) + \text{higher order terms}, \tag{76}$$

obtained by expanding the logarithm in equation (41) and inserting the definition of s_1 from equation (42). In the unconstrained case we have $\lambda_s = \lambda_2$, but for the constrained models one of the other two eigenvalues of the matrix $\mathbf{Q}$ has a larger absolute value so long as $x \neq 0$ or $y \neq 0$. For example, if x and y are both positive, then $\lambda_s = \lambda_4$ and the leading-order corrections for the unconstrained, even and odd models are

$$\langle m \rangle_u - s_1 = -2s_1 \left(\frac{\lambda_2}{\lambda_1}\right)^N, \tag{77}$$

$$\langle m \rangle_{\mathrm{e}} - s_1 = -\langle m \rangle_{o,N} + s_1 = (c_1 - s_1) \left(\frac{\lambda_4}{\lambda_1}\right)^N, \tag{78}$$

J. Stat. Mech. (2015) P03004

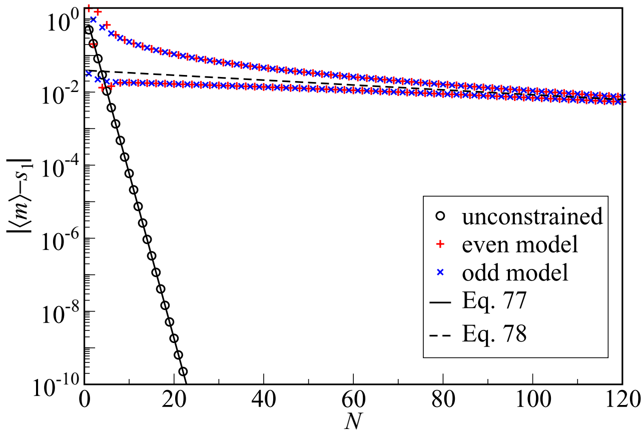

Figure 5. The difference between the magnetization $\langle m\rangle$ and s_1 for a finite chain of length N, $x = 0.5$ and $y = 1$. We note that s_1, defined in equation (42), is the thermodynamic limit of $\langle m\rangle$. Circles, $+$ and $\times$ symbols are exact results. The solid and dashed lines are the leading-order approximations of equations (77) and (78). The constrained models converge much more slowly than their unconstrained counterpart.

respectively (see equation (43) for the definition of c_1). In general, $|\lambda_4|$ is considerably larger than $|\lambda_2|$. As a consequence, the leading-order correction decays much more slowly in the constrained cases than in the unconstrained one (figure 5).

The difference in the asymptotic approach to the thermodynamic limit becomes even more apparent if we take the limit $N \to \infty$ while simultaneously $J \to \infty$ (so that $T_\mathrm{r} \to 0$) and $H \to 0$ (so that $x \to 0$) in such a way that the products

$$t \equiv N T_\mathrm{r}, \tag{79}$$

$$h \equiv N \sinh x \tag{80}$$

are constants. In the thermodynamic limit the magnetic field H scales $\propto N^{-1}$. We could have alternatively defined $h = Nx$ to make this inverse proportionality more apparent, but the definition of equation (80) is a little bit more convenient when substituting the hyperbolic functions in equations (37) and (38). After applying the formula $\lim_{N\to\infty}(1 + z/N)^N = \mathrm{e}^z$ to equations (39) and (40), we obtain the partition functions for large N,

$$Z_u = 2N^{N/2} t^{-N/2} \cosh\sqrt{h^2 + t^2}, \tag{81}$$

$$Z_{e,o} = \begin{cases} N^{N/2} t^{-N/2} \left(\cosh\sqrt{h^2+t^2} \pm \cosh h\right) & \text{if } N \text{ is even,} \\ N^{N/2} t^{-N/2} \left(\cosh\sqrt{h^2+t^2} \mp \sinh h\right) & \text{if } N \text{ is odd.} \end{cases} \tag{82}$$

All thermodynamic quantities can now be derived from the partition function by taking the appropriate derivatives, for example $\langle m\rangle = \partial(\ln Z)/\partial h$. Alternatively, we can also take the thermodynamic limits of equations (44), (48) and (60). We tabulate the results in table 1.

It is instructive to compare these equations with the canonical finite-size scaling forms, for example for the susceptibility

$$\chi(h = 0) \propto N^{\gamma/\nu} f_\chi(N^{1/\nu} t). \tag{83}$$

J. Stat. Mech. (2015) P03004

Table 1. Thermodynamic properties for $N \to \infty$ and constant t, h (defined in equations (79) and (80)).

<table>
<tr><th></th><th>Unconstrained</th><th>Even model</th><th>Odd model</th></tr>
<tr><td>$\langle m\rangle$</td><td>$\frac{h\tanh\sqrt{h^2+t^2}}{\sqrt{h^2+t^2}}$</td><td>$\frac{\frac{h}{\sqrt{h^2+t^2}}\sinh\sqrt{h^2+t^2}+\sinh h}{\cosh\sqrt{h^2+t^2}+\cosh h}$</td><td>$\frac{\frac{h}{\sqrt{h^2+t^2}}\sinh\left(\sqrt{h^2+t^2}\right)-\sinh h}{\cosh\left(\sqrt{h^2+t^2}\right)-\cosh h}$ if N is even,</td></tr>
<tr><td></td><td></td><td>$\frac{\frac{h}{\sqrt{h^2+t^2}}\sinh\sqrt{h^2+t^2}-\cosh h}{\cosh\sqrt{h^2+t^2}-\sinh h}$</td><td>$\frac{\frac{h}{\sqrt{h^2+t^2}}\sinh\left(\sqrt{h^2+t^2}\right)+\cosh h}{\cosh\left(\sqrt{h^2+t^2}\right)+\sinh h}$ if N is odd.</td></tr>
<tr><td>$\frac{\chi(h=0)}{\beta}$</td><td>$\frac{N\tanh t}{t}$</td><td>$N\left(\frac{\tanh\left(\frac{t}{2}\right)}{t}+\frac{1}{2\cosh^2\left(\frac{t}{2}\right)}\right)$</td><td>$N\left(\frac{\coth\left(\frac{t}{2}\right)}{t}-\frac{1}{2\sinh^2\left(\frac{t}{2}\right)}\right)$ if N is even,</td></tr>
<tr><td></td><td></td><td colspan="2">$N\left(\frac{\tanh t}{t}-\frac{1}{\cosh^2 t}\right)$ if N is odd.</td></tr>
<tr><td>$\frac{C(h=0)}{k_{\mathrm{B}}\beta^2J^2}$</td><td>$\frac{4t}{N}\left(\tanh t+\frac{t}{\cosh^2 t}\right)$</td><td>$\frac{2t}{N}\left(2\tanh\left(\frac{t}{2}\right)+\frac{t}{\cosh^2\left(\frac{t}{2}\right)}\right)$</td><td>$\frac{2t}{N}\left(2\coth\left(\frac{t}{2}\right)-\frac{t}{\sinh^2\left(\frac{t}{2}\right)}\right)$ if N is even</td></tr>
<tr><td></td><td></td><td colspan="2">$\frac{4t}{N}\left(\tanh t+\frac{t}{\cosh^2 t}\right)$ if N is odd.</td></tr>
</table>

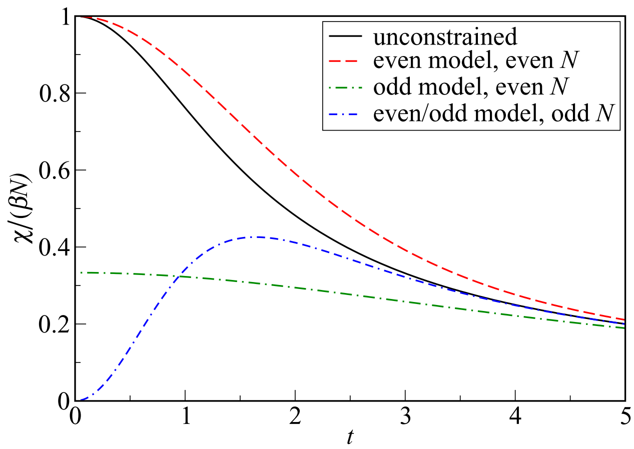

Figure 6. The scaling function of the susceptibility $\chi(h=0)$ in the limit $N \to \infty$, $\beta \to \infty$ with finite $t = N\mathrm{e}^{-2\beta J}$. The scaling functions for the unconstrained, even and odd models exhibit different behaviour, especially if t is small.

While we find that $\gamma = \nu = 1$ for all of the cases listed in table 1 (see also our remark after equation (75)), the scaling functions f_χ (plotted in figure 6) are fundamentally different.

10. The probability distribution of the magnetization

Because of the differences between the unconstrained, even and odd models in table 1, one may wonder how the probability distribution of the magnetization [21–24] differs; after all, $\langle m\rangle$ and χ are essentially the mean and variance of this distribution. We repeat here the arguments developed by Antal *et al* [25] for the unconstrained model with zero magnetic field. We denote the total magnetization by $M \equiv \sum_i \sigma_i$ and the number of domain walls (i.e. boundaries between stretches of contiguous positive and negative spins) by $2d$; it

J. Stat. Mech. (2015) P03004

must be an even number because of the periodic boundary conditions. The main task is to count the number $\Omega(d, M)$ of configurations with $2d$ domain walls and magnetization M. Their probability $P(d, M)$ in thermal equilibrium with $H = 0$ will then follow from

$$P(d, M) = \frac{\mathrm{e}^{(N-4d)y}}{Z}\Omega(d, M), \tag{84}$$

whose marginal distribution

$$P(M) = \sum_d P(d, M) \tag{85}$$

is the probability distribution we are looking for.

We can find $\Omega(d, M)$ with the following combinatorial argument. Let us assume that there are N_+ positive and $N_- = N - N_+$ negative spins and that the first spin is positive. We could for example have

$$\underbrace{w_0+}++\underbrace{w_1-}--\underbrace{w_2+}++\ldots++\underbrace{w_{2d-1}-}w_{2d}+++, \tag{86}$$

where we marked the positions of the domain walls by $w_1, \ldots, w_{2d}$. At the periodic boundary between the first and last spin there may not be a domain wall (in the example above there is not), but we will always symbolically put w_0 in front of the chain. We now mentally glue $w_0, \ldots, w_{2d-1}$ to the next spin in the chain (indicated by the braces in equation (86)). In this manner, d negative spins are attached to domain walls, whereas the remaining $N_- - d$ can be freely placed in the d negative domains. The well-known stars-and-bars theorem [26] implies that there are $\binom{N_- -1}{d-1}$ different ways to distribute the negative spins.

The positive spins require a little more care, because there may not be a positive spin trailing the domain wall w_{2d}. We can account for this exception by not attaching w_{2d} to the following spin. There are thus d positive spins attached to $w_0, w_2, \ldots, w_{2d-2}$, while the remaining $N_+ - d$ positive spins can be freely distributed into $d + 1$ segments, namely the positive intervals following $w_0, w_2, \ldots, w_{2d}$. According to the stars-and-bars theorem, there are $\binom{N_+}{d}$ different possibilities.

Because the positive and negative spins are placed independently of each other, the number of configurations is simply the product of the binomial coefficients $\binom{N_- -1}{d-1}\binom{N_+}{d}$. If we had started the chain with a negative spin, we would have obtained the same expression with the subscripts $+$ and $-$ interchanged, so that

$$\Omega(d, M) = \binom{N_- - 1}{d-1}\binom{N_+}{d} + \binom{N_+ - 1}{d-1}\binom{N_-}{d}. \tag{87}$$

This expression from Antal *et al* [25] is equally valid for the unconstrained, even and odd models. The constraints only enter in the permitted values for M whose consequence becomes apparent when we take the continuum limit. To this end, we take $N \to \infty$ for a fixed value of d and write $m = M/N$, so that

$$\Omega(d, m) = \frac{N^{2d-1}}{2^{2d-2}\, d!\, (d-1)!}\left(1 - m^2\right)^{d-1}. \tag{88}$$

For the time being let us assume that $|m| \neq 1$ and thus $d \neq 0$. We can insert equation (88) into equations (84) and (85), but have to bear in mind that changing from the discrete variable M to the continuous variable m generates an additional prefactor, which we will

J. Stat. Mech. (2015) P03004

call N/Δ_M,

$$P(m)=\frac{4N^{N/2}}{t^{N/2}\Delta_M Z(1-m^2)}\sum_{d=1}^{\infty}\frac{t^{2d}(1-m^2)^d}{2^{2d}d!(d-1)!}. \tag{89}$$

Here Δ_M is the step size between consecutive values of M (i.e. $\Delta_M = 2$ in the unconstrained, $\Delta_M = 4$ in the even and odd models) and t is defined in equation (79). As noticed in [25], the infinite series in equation (89) can be expressed in terms of a modified Bessel function of the first kind thanks to the identity [27]

$$I_1(z)=\sum_{d=0}^{\infty}\frac{z^{2d+1}}{2^{2d+1}d!(d+1)!} \tag{90}$$

and therefore

$$P(m)=\frac{2N^{N/2}I_1\left(t\sqrt{1-m^2}\right)}{t^{N/2-1}\Delta_M Z\sqrt{1-m^2}} \tag{91}$$

for $|m|<1$.

At the boundaries of this interval (i.e. $|m|=1$) there are contributions proportional to Dirac delta functions. These singularities arise because $|m|=1$ implies $d=0$, leaving the denominator in equation (88) undetermined. For the unconstrained model as well as the even and odd models with even N, the proportionality constants in front of the delta functions can be computed based on the observation that $P(m)$ must be normalized and symmetric about $m=0$. For the even model with odd N, a discrete magnetization $M=-N$ is permitted, but $M=N$ is not, so that a delta function can only appear at $m=-1$, but not $m=1$. Conversely, the odd model with odd N can only have a singular contribution at $m=1$, but not at $m=-1$.

The probability contained in the regular part of the distribution given by equation (91) follows from the integral

$$\int_{-1}^{1}\frac{I_1\left(t\sqrt{1-m^2}\right)}{\sqrt{1-m^2}}\,\mathrm{d}m=\frac{4\sinh^2(t/2)}{t} \tag{92}$$

and, upon inserting the partition functions of equations (81) and (82) with $h=0$, we obtain

$$P_u(m)=\frac{tI_1\left(t\sqrt{1-m^2}\right)}{2\sqrt{1-m^2}\cosh t}+\frac{\delta(m-1)+\delta(m+1)}{\cosh t}, \tag{93}$$

$$P_e(m)=\begin{cases}\frac{tI_1\left(t\sqrt{1-m^2}\right)}{4\sqrt{1-m^2}\cosh^2(t/2)}+\frac{\delta(m-1)+\delta(m+1)}{\cosh^2(t/2)} & \text{if } N \text{ is even,}\\ \frac{tI_1\left(t\sqrt{1-m^2}\right)}{2\sqrt{1-m^2}\cosh t}+\frac{2\delta(m+1)}{\cosh t} & \text{if } N \text{ is odd,}\end{cases} \tag{94}$$

$$P_o(m)=\begin{cases}\frac{tI_1\left(t\sqrt{1-m^2}\right)}{4\sqrt{1-m^2}\sinh^2(t/2)} & \text{if } N \text{ is even,}\\ \frac{tI_1\left(t\sqrt{1-m^2}\right)}{2\sqrt{1-m^2}\cosh t}+\frac{2\delta(m-1)}{\cosh t} & \text{if } N \text{ is odd.}\end{cases} \tag{95}$$

One noteworthy detail is that the delta functions peak exactly at the boundaries of the interval $[-1,1]$. So long as the integral of the delta function over the entire real line equals 1, it is a matter of definition how much weight is assigned to the left and right of the

J. Stat. Mech. (2015) P03004

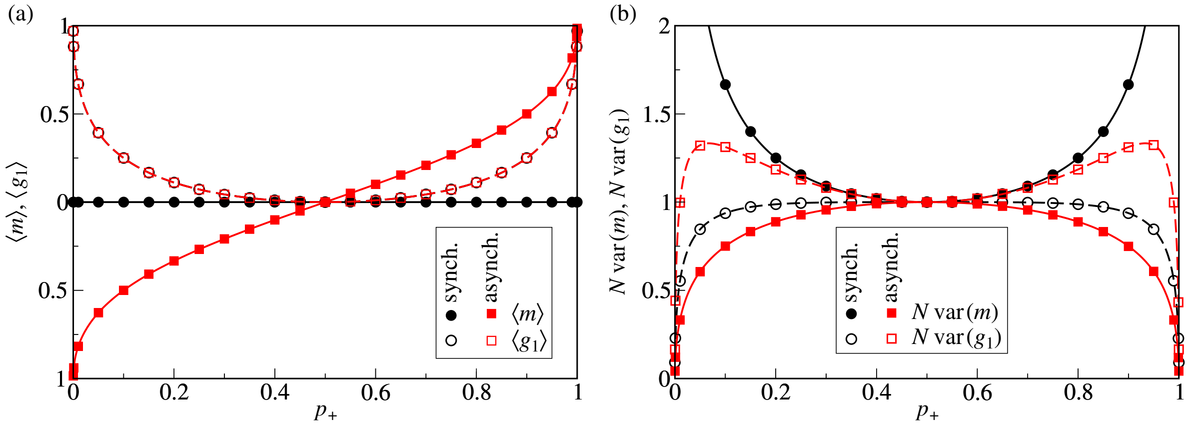

Figure 7. (*a*) Mean nearest-neighbour correlation $\langle m\rangle$ and second-nearest neighbour correlation $\langle g_1\rangle$ in the stochastic voter model. Black curves and symbols are for synchronous, red for asynchronous updates. Analytic predictions (equations (101), (103), (105), (107)) are shown as solid and dashed curves. The results of Monte Carlo simulations for a chain of length $N = 100$ are shown as circles and squares. (*b*) The same for the variances of m and g_1 (equations (102), (104), (106), (108)).

interval boundaries. We have adopted here the symmetric convention $\int_0^\infty \delta(x)\mathrm{d}x = 1/2$ which applies, for instance, if the delta function is the limit of narrowing zero-centred Gaussians. Other conventions are possible; for example [25] implicitly uses $\int_0^\infty \delta(x)\mathrm{d}x = 1$ which changes the prefactors in front of the delta functions in equations (93)–(95). With our definition of the delta function and the integral

$$\int_{-1}^{1} \frac{m^2 I_1\left(t\sqrt{1-m^2}\right)}{\sqrt{1-m^2}}\mathrm{d}m = \frac{2}{t}\left(\frac{\sinh t}{t} - 1\right), \tag{96}$$

we can indeed retrieve the susceptibility χ in table 1.

11. Discussion

Combining the results above, we can now analytically solve the stochastic synchronous and asynchronous voter models introduced in sections 2 and 4. With equation (5) we can translate m and g_1 of the Ising model into correlations between the opinions of nearest and next-nearest neighbours,

$$\langle m\rangle = \frac{1}{N}\left\langle \sum_i \omega_i\omega_{i+1}\right\rangle, \tag{97}$$

$$\langle g_1\rangle = \frac{1}{N}\left\langle \sum_i \omega_i\omega_{i+2}\right\rangle, \tag{98}$$

where the second equation follows from equation (50) and $\omega_{i+1}^2 = 1$. The variances of m and g_1 are proportional to the second partial derivatives of $\ln Z$ with respect to either x

J. Stat. Mech. (2015) P03004

or y, thus

$$N\,\mathrm{var}(m) = \frac{\chi}{\beta}, \tag{99}$$

$$N\,\mathrm{var}(g_1) = \frac{1}{N}\frac{\partial^2}{\partial y^2}\ln Z, \tag{100}$$

where the derivative in the last equation has to be evaluated at $x = 0$ for synchronous and $y = 0$ for asynchronous updates. For synchronous updates, we have in fact evaluated this derivative already in equation (60) because in this case $N\mathrm{var}(g_1) = C/(k_\mathrm{B}\beta^2 J^2)$. The corresponding calculation for asynchronous updates can be performed by differentiating the partition functions in equations (39) and (40).

Inserting equation (9) into equations (45), (48), (54) and (60), we obtain for the synchronous voter model in the thermodynamic limit

$$\lim_{N\to\infty}\langle m\rangle = \begin{cases} 1 & \text{if } N \text{ is odd and either } p_+ = 0 \text{ or } p_+ = 1,\\ 0 & \text{otherwise,}\end{cases} \tag{101}$$

$$\lim_{N\to\infty}[N\mathrm{var}(m)] = \frac{1}{2\sqrt{p_+p_-}}, \tag{102}$$

$$\lim_{N\to\infty}\langle g_1\rangle = \frac{1-2\sqrt{p_+p_-}}{1+2\sqrt{p_+p_-}}, \tag{103}$$

$$\lim_{N\to\infty}[N\mathrm{var}(g_1)] = \frac{8\sqrt{p_+p_-}}{(1+2\sqrt{p_+p_-})^2}, \tag{104}$$

where, as before, $p_- = 1 - p_+$. For asynchronous updates the corresponding results are

$$\lim_{N\to\infty}\langle m\rangle = \frac{\sqrt{p_+}-\sqrt{p_-}}{\sqrt{p_+}+\sqrt{p_-}}, \tag{105}$$

$$\lim_{N\to\infty}[N\mathrm{var}(m)] = \frac{4\sqrt{p_+p_-}}{1+2\sqrt{p_+p_-}}, \tag{106}$$

$$\lim_{N\to\infty}\langle g_1\rangle = \frac{1-2\sqrt{p_+p_-}}{1+2\sqrt{p_+p_-}}, \tag{107}$$

$$\lim_{N\to\infty}[N\mathrm{var}(g_1)] = \frac{16\sqrt{p_+p_-}(1-\sqrt{p_+p_-})}{1+4\sqrt{p_+p_-}(1+\sqrt{p_+p_-})}. \tag{108}$$

We plot equations (101)–(108) in figure 7. As a numerical confirmation we include the results of Monte Carlo simulations in the same graphs. The numerical and analytic results are in excellent agreement.

Comparing the synchronous with the asynchronous case, we notice that the thermodynamic limits of the nearest-neighbour correlations $\langle m\rangle$ differ significantly. While for synchronous updates nearest neighbours are typically uncorrelated, asynchronous updates build up non-zero correlations. Interestingly, the mean second-nearest neighbour correlations $\langle g_1\rangle$ are identical for both update rules. However, the variances differ between the rules: $\mathrm{var}(m)$ is larger for synchronous updates, whereas $\mathrm{var}(g_1)$ is larger for asynchronous updates.

It is in principle possible to extend the calculations to correlations between more distant neighbours too. For example, $\langle \sum \omega_i \omega_{i+3} \rangle$ can be obtained by formally introducing a three-spin interaction strength K in the Hamiltonian so that $E(\boldsymbol{\sigma}) = -K \sum_i \sigma_i \sigma_{i+1} \sigma_{i+2} - J \sum_i \sigma_i \sigma_{i+1} - H \sum \sigma_i$. The mean third-nearest neighbour correlation follows from differentiating the partition function Z with respect to K and subsequently setting $K = 0$ as well as $H = 0$ for synchronous, $J = 0$ for asynchronous updates. Unfortunately, the transfer matrix method developed in section 5 does not easily generalize to arbitrary k-spin interactions [28], but calculating correlations in the voter model from Ising-like Hamiltonians is an intriguing possibility for future research.

12. Conclusion

We have studied two variants of the one-dimensional Ising model: in the first variant the number of positive spins is constrained to an even number; in the second model this number must be odd. We have motivated both models by mapping them to a model of opinion dynamics with either synchronous or asynchronous updates. If the temperature and magnetic field are held constant, the thermodynamic limits of the even and odd Ising models are the same as the limit of the unconstrained model. However, by simultaneously increasing the chain length and lowering the temperature and magnetic field, we have shown that the scaling functions for the even, odd and unconstrained models differ. The mapping from the Ising model has allowed us to obtain explicit formulae for correlations between nearest and next-nearest neighbours in the voter model.

We can generalize the problem posed in this paper to higher dimensions or complex networks by associating spins with the links and enforce an even number of positive spins on every cycle in the graph. In other words, only balanced signed graphs [29] are permitted. Assigning opinions to the nodes and mapping them to spins on the links as in equation (5) will naturally generate such graphs from the voter model. It is a fascinating question how this changes the thermodynamic limits compared to the unconstrained model.

Acknowledgments

This research is supported by the European Commission (project number FP7-PEOPLE-2012-IEF 6-4564/2013). We thank Z Rácz for helpful discussions.

References

[1] Ising E 1925 Beitrag zur Theorie des Ferromagnetismus *Z. Phys.* **31** 253–8
[2] Baxter R J 1982 *Exactly Solved Models in Statistical Mechanics* (London: Academic)
[3] Grosso G and Parravicini G P 2000 *Solid State Physics* (San Diego: Academic)
[4] Schneidman E, Berry M J II, Segev R and Bialek W 2006 Weak pairwise correlations imply strongly correlated network states in a neural population *Nature* **440** 1007–12
[5] Stauffer D 2008 Social applications of two-dimensional Ising models *Am. J. Phys.* **76** 470–3
[6] Siegert A J F and Vezzetti D J 1968 On the Ising model with long-range interaction *J. Math. Phys.* **9** 2173–93
[7] Sherrington D and Kirkpatrick S 1975 Solvable model of a spin-glass *Phys. Rev. Lett.* **35** 1792–6

[8] Ashkin J and Teller E 1943 Statistics of two-dimensional lattices with four components *Phys. Rev.* **64** 178–84
[9] Fernández-Gracia J, Eguíluz V M and San Miguel M 2013 Timing interactions in social simulations: the voter model *Temporal Networks* ed P Holme and J Saramäki (Berlin: Springer) pp 331–52
[10] Skorupa B, Sznajd-Weron K and Topolnicki R 2012 Phase diagram for a zero-temperature Glauber dynamics under partially synchronous updates *Phys. Rev.* E **86** 051113
[11] Newman M E J and Barkema G T 1999 *Monte Carlo Methods in Statistical Physics* (Oxford: Oxford University Press)
[12] Sznajd-Weron K and Krupa S 2006 Inflow versus outflow zero-temperature dynamics in one dimension *Phys. Rev.* E **74** 031109
[13] Wolfram S 1983 Statistical mechanics of cellular automata *Rev. Mod. Phys.* **55** 601–44
[14] Nowak M A, Bonhoeffer S and May R 1994 Spatial games and the maintenance of cooperation *Proc. Natl Acad. Sci.* **91** 4877–81
[15] Gracia J F, Eguíluz V M and Miguel M S 2011 Update rules and interevent time distributions: slow ordering versus no ordering in the voter model *Phys. Rev.* E **84** 015103
[16] Varga L, Vukov J and Szabó G 2014 Self-organizing patterns in an evolutionary rock-paper-scissors game for stochastic synchronized strategy updates *Phys. Rev.* E **90** 042920
[17] Godfray H C J and Hassell M P 1989 Discrete and continuous insect populations in tropical environments *J. Anim. Ecol.* **58** 153–74
[18] Gallegati M, Keen S, Lux T and Ormerod P 2006 Worrying trends in econophysics *Physica* A **370** 1–6
[19] Kramers H A and Wannier G H 1941 Statistics of the two-dimensional ferromagnet. Part I *Phys. Rev.* **60** 252–62
[20] Nelson D R and Fisher M E 1975 Soluble renormalization groups and scaling fields for low-dimensional Ising systems *Ann. Phys.* **91** 226–74
[21] Bruce A D 1981 Probability density functions for collective coordinates in Ising-like systems *J. Phys. C: Solid State Phys.* **14** 3667–88
[22] Bruce A D 1985 Universality in the two-dimensional continuous spin model *J. Phys. A: Math. Gen.* **18** L873–7
[23] Zheng B 2003 Generic features of fluctuations in critical systems *Phys. Rev.* E **67** 026114
[24] García-Pelayo R 2009 Distribution of magnetization in the finite Ising chain *J. Math. Phys.* **50** 013301
[25] Antal T, Droz M and Rácz Z 2004 Probability distribution of magnetization in the one-dimensional Ising model: effects of boundary conditions *J. Phys. A: Math. Gen.* **37** 1465–78
[26] Feller W 1950 *An Introduction to Probability Theory and Its Applications* (New York: Wiley)
[27] Olver F W J 1972 Bessel functions of integer order *Handbook of Mathematical Functions* ed M Abramowitz and I A Stegun, 9th edn (New York: Dover)
[28] Fan Y 2011 One-dimensional Ising model with k-spin interactions *Eur. J. Phys.* **32** 1643–50
[29] Harary F 1953 On the notion of balance of a signed graph *Michigan Math. J.* **2** 143–6
[30] Villain J 1977 Spin glass with non-random interactions *J. Phys. C: Solid State Phys.* **10** 1717–34

J. Stat. Mech. (2015) P03004